ELSEVIER

Journal of Structural Geology 27 (2005) 769–780

JOURNAL OF STRUCTURAL GEOLOGY

www.elsevier.com/locate/jsg

Fault reactivation control on normal fault growth: an experimental study

Nicolas Bellahsen[a,b,*], Jean Marc Daniel[a]

[a]*Institut Français du Pétrole, Rueil Malmaison, France*
[b]*Université Pierre et Marie Curie, Paris 6, France*

Received 19 August 2003; received in revised form 29 October 2004; accepted 7 December 2004
Available online 14 March 2005

Abstract

Field studies frequently emphasize how fault reactivation is involved in the deformation of the upper crust. However, this phenomenon is generally neglected (except in inversion models) in analogue and numerical models performed to study fault network growth. Using sand/silicon analogue models, we show how pre-existing discontinuities can control the geometry and evolution of a younger fault network. The models show that the reactivation of pre-existing discontinuities and their orientation control: (i) the evolution of the main fault orientation distribution through time, (ii) the geometry of relay fault zones, (iii) the geometry of small scale faulting, and (iv) the geometry and location of fault-controlled basins and depocenters. These results are in good agreement with natural fault networks observed in both the Gulf of Suez and Lake Tanganyika. They demonstrate that heterogeneities such as pre-existing faults should be included in models designed to understand the behavior and the tectonic evolution of sedimentary basins.

Keywords: Normal faults; Reactivation; Relay faults; Extension; Rift; Gulf of Suez; Lake Tanganyika

1. Introduction

Fault propagation has been studied through field observation, analogue and numerical modeling. These methods have been used to define a growth sequence at the scale of an isolated fault and at the scale of the whole fault network: this growth sequence explains the evolution of throw and length by two main mechanisms, radial propagation and segment connection (Cartwright et al., 1995; Cowie and Scholz, 1992; Marchal et al., 1998; Peacock and Sanderson, 1991). The parameters emphasized to capture the characteristics of fault networks are mainly the characteristics of the homogeneous brittle layer such as the thickness and the mechanical behavior (Cowie and Scholz, 1992; Lavier et al., 1999; Vendeville et al., 1987). However, other controlling parameters such as fault reactivation are known to be important, as shown by several pieces of field evidence (see Morley, (1999) for a review). For example, in both the Gulf of Suez and the Lake Tanganyika rifts (East African rifts), geological evidence shows that earlier fault networks were reactivated during rifting (see below for references).

Despite these pieces of evidence, fault reactivation and the presence of pre-existing structural heterogeneities are generally neglected in analogue and numerical models of crustal extension. Analytical studies on reactivation (Ranalli and Yin, 1990; Yin and Ranalli, 1992) highlighted the importance of pre-existing fault orientation in the stress field. They do not take into account the entire fault population and cannot predict the features associated with reactivation, and for example the geometry of the small scale faulting around the reactivated faults. Experiments of oblique rifting on velocity discontinuity show the influence of an underlying oblique pre-existing zone of weakness (Clifton et al., 2000; McClay and White, 1995; Tron and Brun, 1991), especially on the fault orientation distribution. As underlined by Morley (1999), such studies neglect the effect of pre-existing zones of weakness inside the brittle layer. Only a few analogue and numerical models have included the pre-existing faults in a brittle layer. These models deal with basin inversion, thrust tectonics (Sassi et al., 1993), post-compression extension (Faccenna et al.,

* Corresponding author. Now at and correspondence address: Department of Geological and Environmental Sciences, Stanford University, 450 Serra Mall Bldg 320, Stanford, CA 94305-2115, USA. Tel.: +1 650 723 4788x2; fax: +1 650 725 0979.
E-mail address: nicolasb@pangea.stanford.edu (N. Bellahsen).

0191-8141/$ - see front matter © 2005 Elsevier Ltd. All rights reserved.
doi:10.1016/j.jsg.2004.12.003

1995), and successive phases of extension (Bonini et al., 1997; Dubois et al., 2002) but not with reactivation of normal faults in extension. These studies show that reactivation depends not only on dip and strike of the pre-existing faults, but also on the spatial organization on the structural heterogeneities.

The aim of the experiments described in this paper is to define the influence of a pre-existing fault network on the geometry of the resulting normal fault network. We characterize its influence on fault orientation distribution, small faults, and depocenters.

2. Experimental procedure

The analogue models are made of sand representing brittle layers (2 cm thick) and silicone putty representing ductile layers (1 cm thick) (Fig. 1). They are deformed in a box with initial dimensions of $40\times50\times10$ cm^3. The dry sand obeys the Coulomb failure criterion, with a very low cohesion (30 Pa) and a friction angle of 35° (Dubois et al., 2002; Krantz, 1991). The silicon putty is a Newtonian fluid with a viscosity of 5×10^4 Pa s at room temperatures and strain rates of the experiments (Weijermars, 1986). These materials have been repeatedly used for modeling the brittle and ductile deformation of the crust and the scaling relations (see Hubbert, 1937; Davy and Cobbold, 1991) indicate that the length factor is about 10^{-5} (1 cm in the model represents 1 km) and the time factor is about 10^{-10} (1 h represents 1 Ma).

The discontinuities (Fig. 1) are created by the introduction of 0.5-mm-thick and 10-cm-wide pieces of cardboard through the sand layer down to the top of the silicone layer. Their dip is 60° and their strike is at 45 or 70° to the direction of extension. The introduction and removal of the cardboard create a zone of dilation as a result of grain re-arrangements. This zone acts as a zone of weakness and obeys a Coulomb's frictional slip criterion. The coefficient of friction (0.4) (Sassi et al., 1993) of this zone is lower than the internal friction (0.6) of the undisturbed sand (Sassi et al., 1993). The density of the discontinuities is about 50 faults per meter square. This density was mainly decided by practical reasons: spacing should not be too small to avoid perturbing a discontinuity when creating another one, spacing should not be too high to observe some fault interactions. The spacing of pre-existing faults in nature is difficult to estimate. Thus, we did not really try to simulate a particular natural spacing. In this study, a basal rubber sheet transmits the extension to the overlying materials and induces a quite homogeneous extension. The models have been chosen for their similarity with the conditions inside a rift, while at the scale of the whole rift, the basal conditions are often considered as a velocity discontinuity (Allemand and Brun, 1991; Brun, 1999; Michon and Merle, 2000). Furthermore, the models allow the intrinsic role of discontinuities inside the brittle layer to be examined without the influence of underlying discontinuities. The experiments are analyzed using photographs and time lapse topography of the models (laser acquisition with a resolution of $0.25\times0.25\times0.25$ mm). The topographic information is used to compute fault throw at the surface.

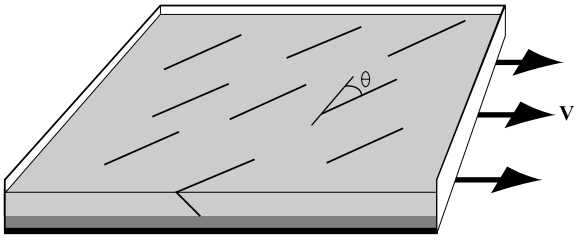

Fig. 1. Experimental setup. The models are composed of two layers, one sand layer representing brittle layers and one silicone layer that represents a viscous layer. The discontinuities are introduced by the introduction of a 10-cm-long piece of cardboard, with a dip around 60°. The extension is transmitted through the base of the model and the stretching of a basal rubber sheet.

3. Results

The four experiments described below have been selected from a set of 20 experiments to highlight the role of the pre-existing discontinuity orientation and the consequences of fault reactivation at the scale of the complete fault network.

3.1. Experiment 1: reference experiment

The first experiment (Fig. 2) is an experiment without discontinuities (the layers are homogeneous). This experiment is briefly described and considered as a reference experiment. This experiment is a classical one, where sand and silicone are subjected to a basal extension. In this experiment, faults grow as detailed in many previous studies (Cartwright et al., 1995; Cowie and Scholz, 1992; Marchal et al., 1998; Peacock and Sanderson, 1991; Bellahsen et al., 2003). The fault segment connection occurs after interaction between two segments: one (or both) curves to connect to the other or secondary faulting occurs in the relay ramp (Fig. 2). In each case, the young relay segment fault has a throw smaller than the two older segments, which produces irregular throw profiles after connection. The throw minima can be about 50% of the maximum throw and are located at the linkage point (Childs et al., 1995; Peacock and Sanderson, 1991; Trudgill and Cartwright, 1994; Willemse et al., 1996).

The fault segments are counted as a function of their orientation. A fault segment is defined by its propagation mechanism (growth of a fault by lateral tip propagation) and its orientation. In experiment 1, the distribution of the fault segment orientation is unimodal, perpendicular to the extension direction, as shown in several previous studies (Clifton et al., 2000; Tron and Brun, 1991). During the

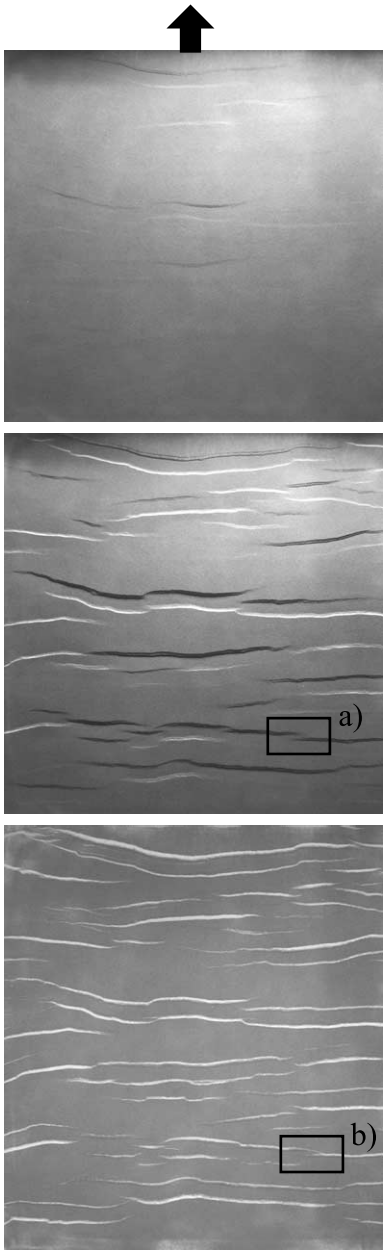

Fig. 2. Experiment 1: homogeneous brittle layer experiment after 3, 8, and 14% extension. The faults grow as described in the literature: by lateral propagation of the fault tips, and by connection of segments. The geometry and the connection in a relay ramp are illustrated by the two squares on the figure. One segment turns to connect to the other one and the resulting fault presents a characteristic undulation and throw deficit.

extension process, the total fault segment number does not increase linearly (Fig. 3a). After 2–3% extension, several faults initiate; the rate of segment initiation increases from 2 to 15 per percent of extension (Fig. 3b). Between 4 and 5% extension, the rate of segment initiation is greatest. From this point, the rate decreases, attaining a value of 5 after 6% extension. At around 6–11%, the rate of segment initiation is quite constant (around 5), and the number of segments then increases constantly.

3.2. Experiment 2

In this experiment, discontinuities are introduced in the brittle layer. The angle between the discontinuity strike and the direction of extension is 70°. The pre-existing discontinuities are reactivated and propagate from their extremities perpendicular to the extension direction (Fig. 4). In the first stages of extension (0–5%), the reactivated faults constitute the main population (Fig. 5), as highlighted by the numerous faults segments striking at 110–120° (the extension direction is N–S). With increasing extension, these segments continue to accommodate a large part of the applied extension, and their number increases constantly, attaining almost 20 (Fig. 5). The segments perpendicular to extension tend to become the major fault population (Fig. 5). However, the reactivated segments still constitute an important fault population. Their number increases and is high during the experiment. The reactivated faults and their propagated segments constitute the main faults of the network and the distribution of segments orientation is bimodal. Reactivated faults, during their propagation, can connect to each other through segments perpendicular to the extension (a in Fig. 4) or by an oblique segment if they are close enough to each other (b in Fig. 4b).

The number of fault segments (Fig. 3a) increases quite constantly during the first 15% extension to 85 fault segments. This evolution is the first difference with respect to the reference experiment, which shows a significant increase after 5% extension. However, from 5 to 6% extension, the evolution of the number of fault segments is similar in the two experiments (experiments 1 and 2, increasing from around 25 to 85 in 10% extension) as well as the rate of initiation (Fig. 3b).

3.3. Experiment 3

In this experiment, the angle between the discontinuity strike and the extension is 45°. Due to this angle, the pre-existing discontinuities are less prone to reactivation than those of experiment 2. Looking at the fault network, one may note that the reactivated fault density is not strictly the same as the previous experiment. This was due to model construction issues; we were trying to keep the same kind of overlap between the discontinuities. We are conscious that it may influence the results of the experiment. However, we think that it does not influence the fault status (main or relay fault) but only the way the faults interact. As in the previous experiment, deformation is first located at the pre-existing fault extremities (Fig. 6). During the early stages, the reactivated faults acquire a significant throw and propagate perpendicular to the applied extension. The number of reactivated segments is around 10 and the number of newly created ones (commonly their propagation) is around 7 at 2% extension (Fig. 7). Due to their orientation, the reactivated faults cannot accommodate the whole applied extension and therefore new faults initiate. With increasing

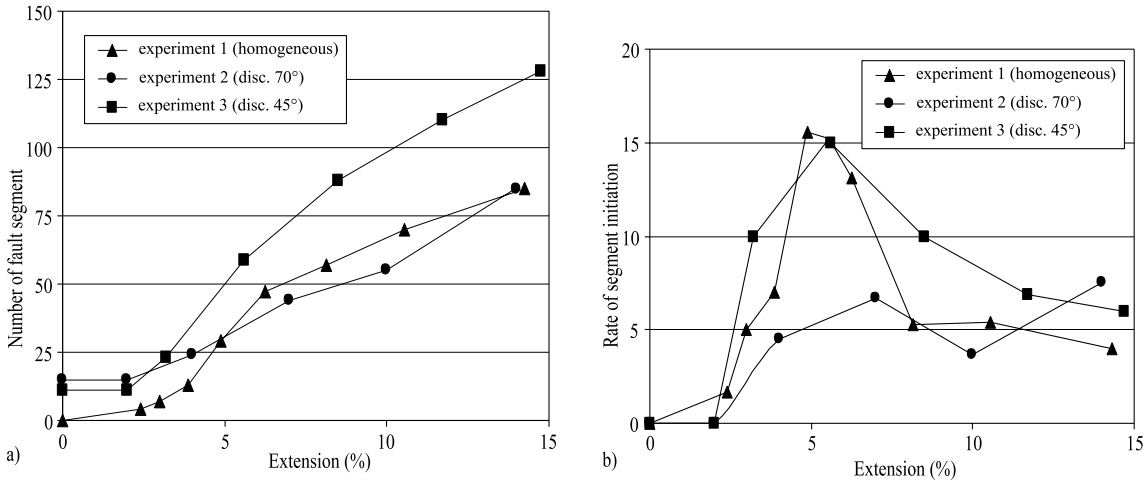

Fig. 3. Fault segment numbers for experiments 1–3. The fault segments are counted for several steps of the three first experiments. The numbers of segments are similar for the homogeneous experiment and with discontinuities at high angle to the extension. However, in the experiment with discontinuities at low angle to the extension, the number of segments is larger.

extension, these newly created faults and the propagated segments of the reactivated discontinuities accommodate a great part of the applied extension. As shown on Fig. 7, a bimodal distribution of fault segment orientation develops. The number of newly created faults (perpendicular to the direction of extension) tends to become more important, progressively forming the major fault population to reach 50 segments. The population of the reactivated discontinuities does not increase in number (Fig. 7), and they form relay faults in the final fault network (Fig. 6). They are perfectly oriented to transfer deformation between newly created faults. The orientation distribution is bimodal (as in the previous experiment), but here the population of segments perpendicular to extension is more important than the oblique segments.

In this experiment, the number of fault segments (Fig. 3a) is greater than in the two first experiments. This number attains a value of 125 after 15% extension while it attains 85 in experiments 1 and 2. This makes a very segmented deformation. However, the rate of segment initiation (Fig. 3b) evolves in a similar way to experiment 1. The rate increases after 2% extension, attaining a value of 15 segments per percent of extension. After the peak of segment initiation, the rate decreases less than that found in experiment 1. After 15% extension, it attains a rate similar to experiment 2, around 5 segments per unit percent of extension. This shows that, at the scale of the whole fault network and from a statistical point of view, the reactivation does not play a very important role (except at the beginning of the experiment). The fault network, after 5% extension, behaves quite similarly to the one generated in a homogeneous brittle layer.

The reactivated faults are not active during the whole experiment and along their entire length. Because they are used as relay faults, they are active along a small portion of their length. However, even if some reactivated segments are inactive (or slightly active), they significantly perturb the lateral propagation of newly created faults. In some cases, the lateral propagation can be inhibited. In other cases, this propagation can be deviated, following the discontinuity. Finally, the inactive part of the discontinuity can be cut by new faults that are laterally propagating toward them.

3.4. Experiment 4

In this experiment, after the introduction of the discontinuities and before the extension, an additional 2-cm-thick sand layer was added to the model. The pre-existing discontinuities are at 45° the extension direction, as in experiment 3 (Fig. 8). This model setup allows us to study not only the lateral propagation but also the vertical propagation of the reactivated faults.

The first brittle layer represents the basement and the second the cover. This experiment also simulates brittle layers strongly coupled in the sense that there is no ductile level between them. This experiment shows the propagation of reactivated oblique basement fault in the sedimentary cover in the case of strong coupling (Fig. 8). In the first stage of extension, the reactivated faults are more segmented than in the previous experiment and the segment orientations are closer to the extension direction. With increasing extension, these segments connect to each other to form a relay fault parallel to the underlying basement fault. The fault pattern is very similar to that in experiment 3.

4. Discussion and comparison with natural fault systems

In summary, we have shown the strong influence of a pre-existing fault network obliquely reactivated in extension. We are conscious that one limitation of the method is

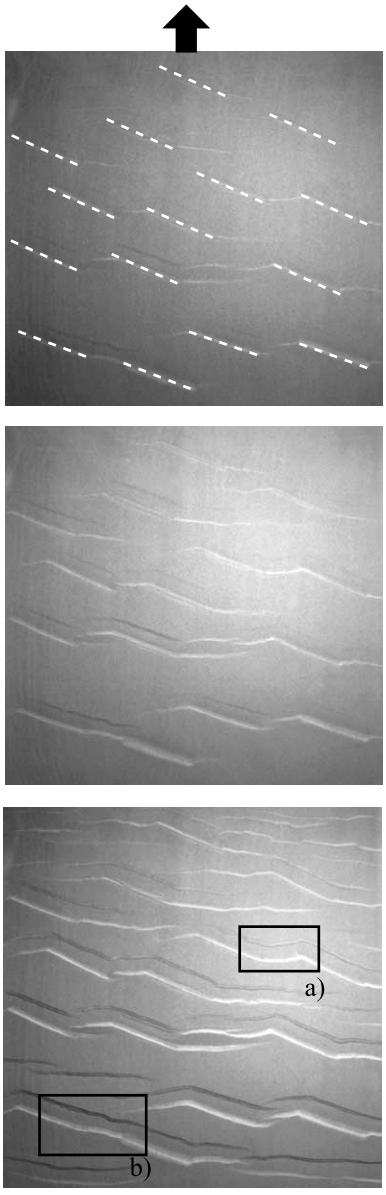

Fig. 4. Experiment 2: the pre-existing faults are at 70° to the extension direction after 2, 5, and 14% extension. The faults are reactivated and accommodate a great part of the applied extension. Most of the main faults, secondary faults and grabens are oblique to the extension direction. The reactivated faults propagate through a segment perpendicular to the applied extension (a) or through an oblique segment (b).

that we did not investigate the influence if there was a relative weakness of the discontinuity. In these experiments, the reactivation is strongly favored by the structure of the discontinuity itself. Introducing and removing the cardboard in the sand, we produce a zone of dilatancy but also probably a zone of surrounding contraction. This porosity contrast may be slightly different than in nature. However, we believe that the results of the experiments may provide some guides to our structural interpretation of fault networks. This influence is especially dependant on the strike of the reactivated faults. We now discuss these results

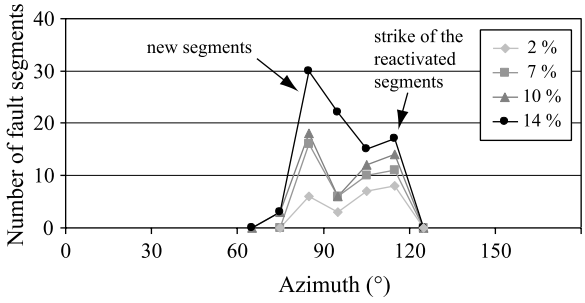

Fig. 5. Distribution of orientation of the fault segments in experiment 2. The distribution is bimodal. One population represents the reactivated segments and is dominant at the beginning of the experiment until around 3% extension. The second population is the newly created segments, which becomes dominant after 5% extension. However, the two populations of segments are important and increase in number during the whole experiment. Some fault segments that have the same strike than reactivated ones are not reactivated. (This explains why on the diagram we see more segments around 115° than on Fig. 4.)

in the light of two natural examples where fault reactivation may have occurred during the rifting stage. These examples are compared with the analogue experiment results.

4.1. Natural examples

In the Gulf of Suez rift, consequences of oblique reactivation can be illustrated. This Oligo-Miocene rift (Fig. 9) is controlled by 150° (N150°E) striking faults (called clysmic faults) and created by a 60° direction of extension (Lyberis, 1988). The main rift orientation is 150° and its half graben geometry is separated along strike by 20° transfer faults (Colletta et al., 1988; Patton et al., 1994). These transfer faults are interpreted as basement discontinuities (Moustafa and Abd-Allah, 1992). The rift, the major faults and the fault-controlled basins are perpendicular to the extension direction, and defined an orthogonal rift (Colletta et al., 1988). However, at smaller scale, the fault network is also comprised by N–S to 20° striking faults. These faults are interpreted as reactivated oblique pre-existing discontinuities (Jarrigue et al., 1990).

The Lake Tanganyika rift (East Africa) is N–S in its northern part (Fig. 10). This rift was active from Miocene times to present. The half graben are controlled by N–S-trending major faults trending 20 and 140°. Pre-rift fabrics are recognized in the areas, trending 140°. They are believed to have been inherited from a Paleoproterozoic orogeny. The 140° Miocene faults are interpreted as reactivated discontinuities and seem to influence the normal fault propagation and depocenter geometry and evolution (Lezzar et al., 2002).

The characteristics of these two rifts are compared with the results of the analogue models of reactivation. The four previous experiments highlight the effect of the normal fault network reactivation during extension. We now discuss a few important consequences of the reactivation: the

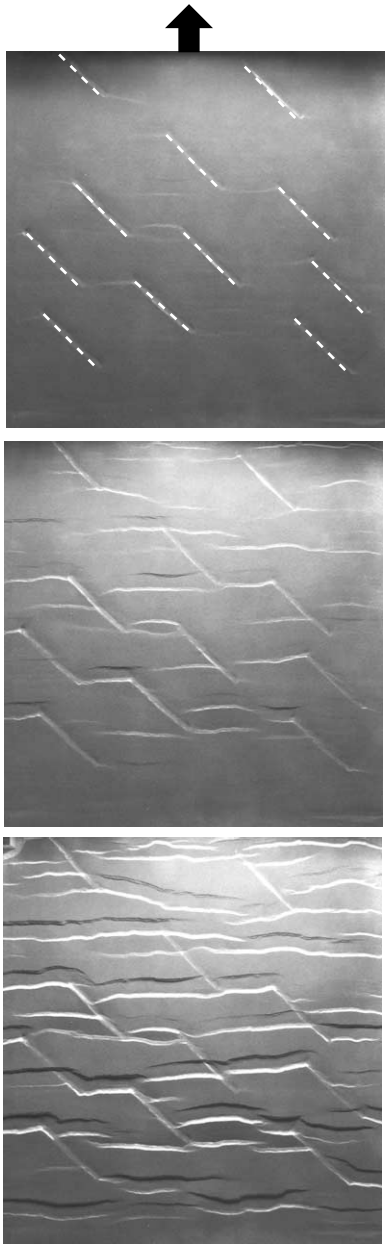

Fig. 6. Experiment 3: the pre-existing faults are at 45° to the extension direction (extensions at 3, 8, and 14%). The faults are reactivated but are used as relay faults (see the square on the figure). The resulting fault pattern presents typical undulations and characteristic throw profile (see text and Fig. 14).

segmentation at the scale of the fault network, the relay fault geometry and the geometry of depocenters.

4.2. Fault orientations and segmentation

The faults obtained in the analogue models of oblique reactivation have a bimodal orientation distribution. However, these distributions have a different evolution through time. When the pre-existing faults are favorably oriented (experiment 2), they are reactivated and form a major fault

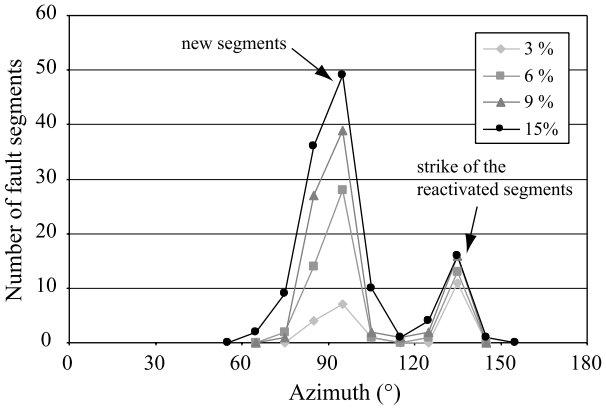

Fig. 7. Distribution of the orientation of the fault segments in experiment 3. The distribution is also bimodal. One population represents the reactivated segments and is dominant at the beginning of the experiment until around 5% extension. The second population is the newly created segments, which becomes dominant after 5% extension. The reactivated population does not increase in number significantly. The initiated segments are mainly segments perpendicular to the extension direction. Some fault segments that have the same strike than reactivated ones are not reactivated. (This explains why on the diagram we see more segments around 135° than on Fig. 6).

segment population with the new perpendicular segments. This is shown by the two peaks of fault segment number (Fig. 5) that are quite similar in amplitude. When the pre-existing faults are at lower angle to the direction of

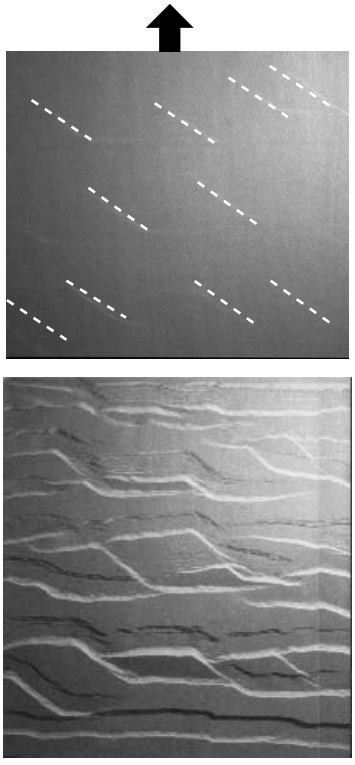

Fig. 8. Experiment 4: the pre-existing faults are at 45° to the extension direction, but a 'post-discontinuities and pre-rift' sand layer is added (extension at 14%). The final fault network is very similar to the one of experiment 3.

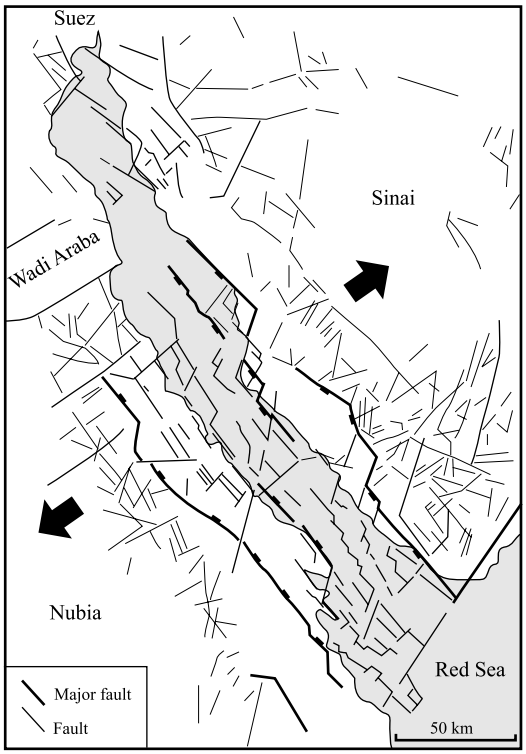

Fig. 9. Structural map of the Gulf of Suez modified from Schütz (1994). The main faults are black. Note the bimodal fault orientation distribution, faults strike 150° and parallel to the rift trend, others strike 20°. Large main faults are composed of 150° striking segments and 20° striking segments.

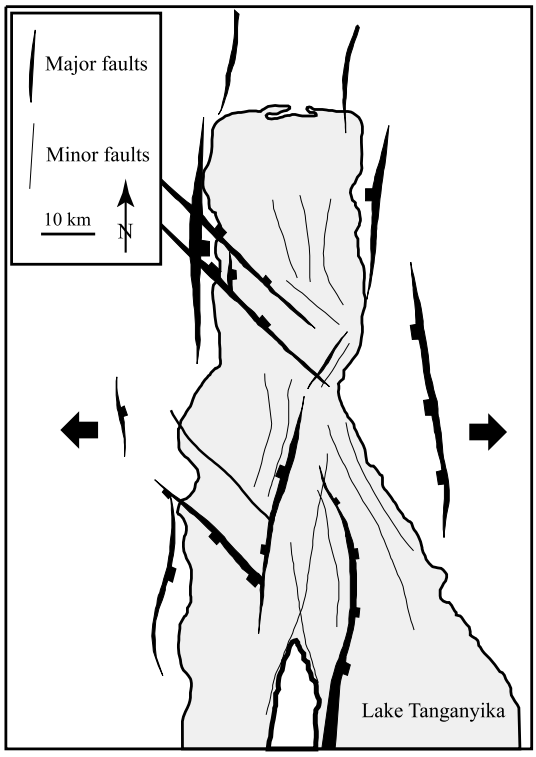

Fig. 10. Schematic structural map of the Lake Tanganyika rift simplified from Lezzar et al. (2002). The faults strike mainly N–S and NW–SE. The NW–SE faults are identified as reactivated faults during the Miocene rifting.

extension (experiment 3; discontinuities at 45°), the reactivated faults form a minor fault population because they are used as relay faults. The fault segment population formed by reactivated segments tends to become a minor population (Fig. 7). Even though these two pre-existing fault networks (at low and high angle to the direction of extension) are reactivated, the resulting fault network is markedly different. These results cannot be predicted by analytical studies or analogue or numerical 2-D models. Analytical studies (Ranalli and Yin, 1990; Yin and Ranalli, 1992) show that reactivation of a unique isolated fault depends on the discontinuity strike and dip with respect to the principal stresses. However, in the field of the possibly reactivated fault strikes, their orientation decides their behavior as main or relay faults.

Recently, Morley et al. (2004) showed how other parameters influence the status of reactivated faults. Increasing the weakness of pre-existing faults, their status changes from minor to major faults. Similarly to what we obtained here, strong pre-existing faults can be reactivated but will form only relay faults for the final fault network. On the contrary, weak faults are reactivated and form main faults.

More generally, reactivation processes segment the fault network. Regarding the fault directions, the reactivation produces segmented composite faults, as they are composed of reactivated and newly created faults. This occurs whatever the reactivated fault orientation. Moreover, when the reactivated faults are at low angle to the direction of extension, the fault segment number is greater than in experiments without pre-existing discontinuities or than in experiments with discontinuities at high angle to the direction of extension. The segmentation is then much more important and is due to the fact that the pre-existing faults are not well oriented. The experiment with pre-existing discontinuities at high angle to the extension is similar to the experiment with a homogeneous brittle layer (except in the first percent extension) from the point of view of the rate of fault initiation.

The reactivation of an oblique fault network in extension has consequences for the fault orientation distribution. This mechanism produces a bimodal distribution as shown on Figs. 7 and 11. The fault orientation distribution of experiment 3 is very similar to the one in the Gulf of Suez published by Colletta et al. (1988) (Fig. 11, and compare Fig. 10 with Fig. 7), in terms of both the segment orientations and their relative numbers. The major population is comprised of segments that strike perpendicular to the extension and the minor population is comprised of reactivated segments at high angle to the extension. This confirms that the faults in the Gulf of Suez can be the result of combination of reactivation and initiation of new faults.

In Lake Tanganyika, the fault orientation distribution is

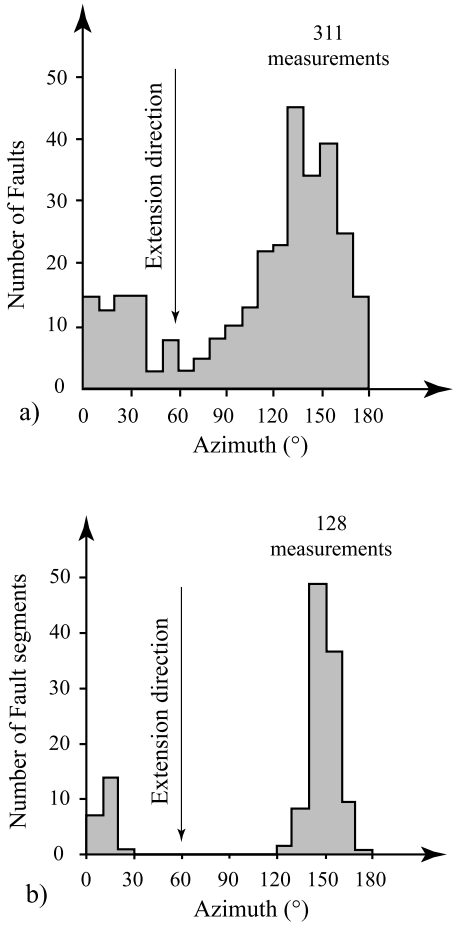

Fig. 11. Distribution of fault orientation in the Gulf of Suez (Colletta et al., 1988) and in experiment 3 (after 15% extension). The two distributions are similar, one peak is quite perpendicular to the direction of extension, another one is strongly oblique at around 45°.

also clearly bimodal. Lezzar et al. (2002) showed that the influence of the reactivated faults tends to decrease during rift evolution. In the early stages, both the reactivated oblique faults and the newly created orthogonal faults control the rift structure and sedimentation. In the later stages, the newly created faults tend to form the major population. Experiment 3 could be an analogue as it shows that the reactivated population becomes less important compared with the newly created one (Fig. 7).

Bimodal distributions that are obtained here in a similar setting to orthogonal rifts frequently characterize oblique rifting. This kind of orientation distribution has been used to determine the amount of obliquity between the rift axis and the extension direction. From a natural example, assuming the rift trend and calculating the orientation distribution, Brun and Tron (1993) deduced the direction of extension. The analogue models described here show that a bimodal distribution can occur even in an orthogonal rift. These relations between orientation distribution and rift obliquity have then to take into account the structural inheritance or have to be applied on a fault network growing in a homogeneous brittle layer. Brittle layers (in continental crust) are certainly not homogeneous due to the tectonic inheritance and it is certainly more appropriate to remove the reactivated populations before applying the described method. On the contrary, it can successfully be applied to the oceanic crust (Dauteuil and Brun, 1993), which is young, unperturbed and homogeneous.

4.3. Fault interaction and depocenters

The fault propagation is strongly controlled by the presence of the pre-existing discontinuities. When the discontinuities are at 45° to the extension (experiment 3), different fault interactions are observed, depending on the fault dip direction.

When the reactivated and the newly created faults are not dipping in the same direction, the propagation of the newly created faults is inhibited in the vicinity of the reactivated fault. In Fig. 12a, two normal faults (named B and C) propagate toward each other and toward a pre-existing discontinuity (named A) that is slightly reactivated. Both their throw and length increase. However, when they become closer to the reactivated fault (Fig. 12a and b), their lateral propagation is stopped (at least at the tip close to the reactivated fault). The pre-existing faults acts as a stress barrier. Its activity perturbs the stress field, both in terms of orientation of principle stresses and in terms of their magnitude (Willemse, 1997). The stress drop in the vicinity of the fault inhibits the lateral propagation of the faults. In Fig. 12c, the newly created faults seem to propagate across the reactivated one, which is certainly linked to a decrease of the activity of the reactivated segment. This observation can be associated with a previous one, where we noted that reactivated fault activity decreases with increasing extension. These results are in agreement with those obtained at Lake Tanganyika by Lezzar et al. (2002). There, the presence of pre-existing faults controls the propagation of newly created normal faults. For example, when these two kinds of faults are not dipping in the same direction, the propagation of the new fault is inhibited.

When the reactivated and the newly created faults are dipping in the same direction (Fig. 13), they connect and the reactivated fault is used as a relay fault between two major faults. The faults B and B′ on Fig. 13a are connected to the pre-existing faults A and A′, respectively. Whether the newly created faults propagate toward the reactivated faults or propagate from them, they quickly use pre-existing discontinuity as relay faults. They frequently take advantage of only a part of the pre-existing fault and the other part seems inactive. In this case, the active part remains active during the whole experiment (Fig. 13) and can even influence the formation of the antithetic faults that often initiate obliquely to the direction of extension. Again, this observation was made in Lezzar et al. (2002). Connections occur between reactivated and newly created faults and produce undulating normal faults.

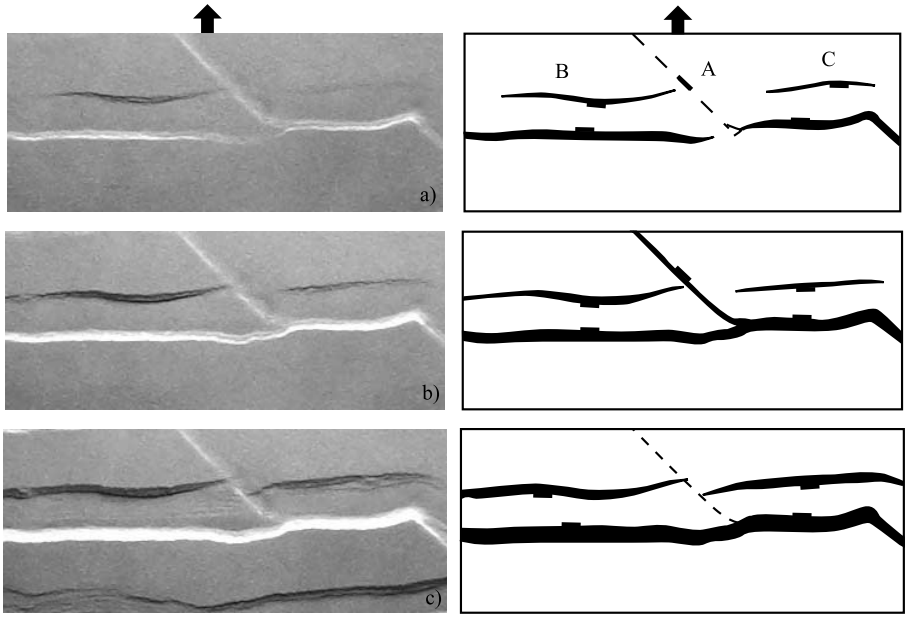

Fig. 12. Fault interaction after (a) 5%, (b) 8%, and (c) 14% extension in the case where the reactivated and new faults are not dipping in the same sense. The new faults B and C propagate toward the reactivated fault A. Their propagation is inhibited as fault A is active and perturbs the stress field. Faults B and C finally propagate through fault A as it becomes inactive.

In experiment 3, the distribution of throw along faults formed by reactivated relay faults is very regular (Fig. 14). Along these faults, topographic lows are present at one of the intersections of the relay fault and the newly created fault, associated with a relative displacement minimum. At the other intersection, the footwall presents a maximum high, associated with the maximum displacement (Fig. 14). The regular throw profile is explained by the fact that there is no linkage event because new faults initiate at the extremities of their future relay fault. The relay ramp has been active since the beginning of the extensional event. Large throws are located at the relay faults and this has important implications for the location of the depocenters that will be located at one of the intersections between reactivated relay faults and newly created faults (Fig. 15). Such characteristics have also been recently described in the Lake Tanganyika rift by Lezzar et al. (2002). The early depocenters are controlled by the reactivated fault segments. Usually in a homogeneous brittle layer, as in experiment 1, where faults connect and a relay initiates, a significant low in throw is recorded. As a consequence, the early depocenters are located where the throw is maximum, i.e. at the center of the fault segments (see for example Gawthorpe and Leeder (2000)) (Fig. 15).

The evolution of the deformation in a relay zone then depends on the presence of pre-existing discontinuities. If the relay fault is a reactivated one, the deformation is accommodated early by a single fault, which accommodates the transfer of deformation between the two major faults. On the contrary, when the relay segment is newly created by two major segments interacting, the deformation is accommodated by small fault segments. The connectivity through time is then different. The relay ramp in the case of the reactivation process is active early and the deformation of the zone is accommodated by a single fault. Similar geometries are found by Morley et al. (2004), where several natural examples from the rifts of Thailand are shown.

4.4. Vertical propagation

In the Gulf of Suez, reactivation occurs in the basement and these faults propagate laterally and vertically toward younger sedimentary layers. Between the basement and the sedimentary cover, ductile layers can induce decoupling, such that the vertical propagation is strongly influenced by the rheology of the system (Higgins and Harris, 1997; Withjack and Callaway, 2000). This decoupling produces strong obliquities between the fault strikes in the basement and fault strikes in the cover. While some reactivated basement faults are oblique, the faults in the sedimentary cover are closer to the perpendicular to the extension direction. In some areas, where a strong decoupling occurs, the influence of reactivation on faulting in the sedimentary cover is then reduced. However, in many areas, the deformation in the basement and the sedimentary cover is strongly coupled, such that fault strikes are parallel to the strike of the oblique basement faults (for example, Abu Durba fault system in the Gulf of Suez (McClay and Khalil, 1998)).

The results obtained in this work are particularly valid in the case of a strong coupling between the basement (where pre-existing discontinuities occur) and the sedimentary cover. These results should be complemented by a similar study with intra-brittle layer decoupling level.

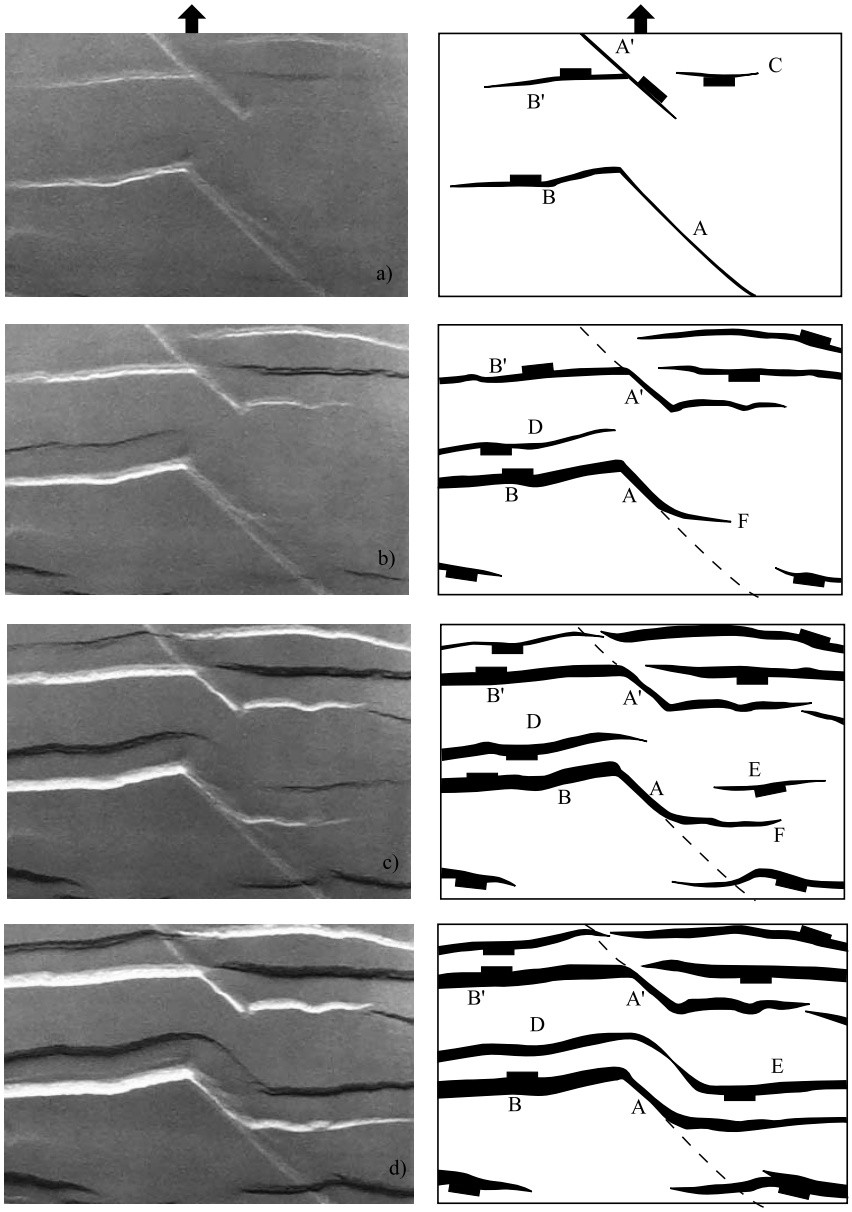

Fig. 13. Fault interaction after (a) 6%, (b) 8%, (c) 11%, and (d) 14% extension in the case where the reactivated and new faults are dipping in the same sense. Faults A and A′ are reactivated, B and B′ are new faults. These last faults propagate toward or from the reactivated ones and then connect to form long and undulating faults. See text for complete description.

5. Conclusions

This work is the first attempt to investigate the effect of a pre-existing oblique normal fault network on the geometry of the younger normal faults, an effect generally neglected in analogue and numerical models. The analogue brittle material (sand) used in our experiments strongly promotes reactivation (low friction coefficient along the pre-existing faults). Therefore, these experiments cannot properly be used to define in which natural conditions reactivation can occur. Nevertheless, the results presented here demonstrate the first order influence of fault reactivation on fault network growth. In particular, fault reactivation and the orientation of the pre-existing discontinuities strongly influence: (i) the geometry of the main faults and the evolution through time of the fault orientation distribution, (ii) the geometry of relay faults, (iii) the secondary faulting associated to the main faults, and (iv) and the location of fault-controlled depocenters.

This work provides some guidelines to detect if oblique fault reactivation was effective during fault growth. The geometry of relay zones, the distribution of throw along the fault and the associated topography reveal the tectonic history of a fault network. The results, coupled to those of Lezzar et al. (2002) and Morley et al. (2004) for example, demonstrate that tectonic models should take into account,

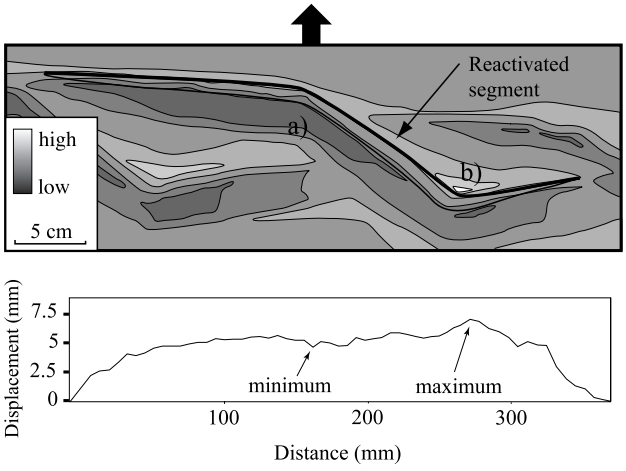

Fig. 14. Normal fault geometries and depocenters in laboratory experiments. The topography and the throw profile of an inherited relay fault in the analogue model are shown. The blue color represents the low altitude and the red the high altitude. The topography low is located in the hanging-wall at the intersection (a) of the relay fault and the main fault. The topographic high is located in the footwall at the other intersection (b). The throw profile is very regular, with maximum and minimum at segment intersections (see text).

more systematically, the role of pre-existing discontinuities when they are known. This work and the natural data cited above now provide new guidelines for structural interpretation of rifted basins. Further experimental work is still required to characterize the role the spatial organization of these discontinuities plays on the final geometry of the fault network. Such work, performed in conjunction with the use of theoretical reactivation criteria in numerical models, should provide a better understanding of deformation mechanisms and tectonic history at various scales, from the rift localization and the major zones of tectonic subsidence to the small scale faulting and geometry of depocenters.

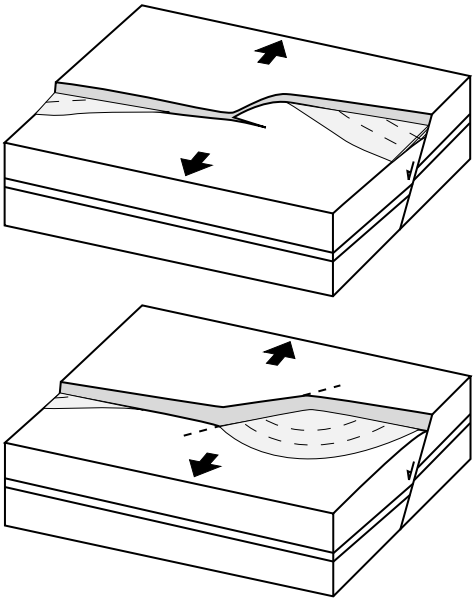

Fig. 15. Idealized fault propagation and associated depocenters in homogeneous and heterogeneous layers. (a) Classical geometry of two connecting segments. The depocenters are located at the center of each segment. They correspond to maxima in the throw profile and minima of the topography. (b) Geometry in the case of a deformed layer with oblique pre-existing discontinuities. The pre-existing fault (dashed line) is used as relay fault. The depocenters are located in the vicinity of the relay zone.

Acknowledgements

The authors would like to thank Bernard Colletta and Laurent Maerten for fruitful discussions and advices. C. Morley, Y. Yamada and the associate editor are thanked for corrections and suggestions that improved the quality of the first version of the paper.

References

Allemand, P., Brun, J.P., 1991. Width of continental rifts and rheological layering of the lithosphere. Tectonophysics 188, 63–69.

Bellahsen, N., Daniel, J.M., Bollinger, L., Burov, E., 2003. Influence of viscous layers on the growth of normal faults: insights from experimental and numerical models. Journal of Structural Geology 25, 1471–1485.

Bonini, M., Souriot, T., Boccaletti, M., Brun, J.P., 1997. Successive orthogonal and oblique extension episodes in a rift zone: laboratory experiments with application to the Ethiopian Rift. Tectonics 16, 347–362.

Brun, J.P., 1999. Narrow rifts versus wide rifts: inferences of rifting from laboratory experiments. Philosophical Transaction of the Royal Society of London 357, 695–712.

Brun, J.P., Tron, V., 1993. Development of the North Viking Graben: inferences from laboratory modelling. Sedimentary Geology 86, 31–51.

Cartwright, J.A., Trudgill, B.D., Mansfield, C.S., 1995. Fault growth by segment linkage: an explanation for scatter in maximum displacement and trace length data from the Canyonlands Grabens of SE Utah. Journal of Structural Geology 17, 1319–1326.

Childs, C., Watterson, J., Walsh, J., 1995. Fault overlap zones within developing normal fault systems. Journal of the Geological Society, London 152, 535–549.

Clifton, A.E., Schlische, R.W., Withjack, M.O., Ackermann, R.V., 2000. Influence of rift obliquity on fault-population systematics: results of experimental clay models. Journal of Structural Geology 22, 1491–1509.

Colletta, B., Le Quellec, P., Letouzey, J., Moretti, I., 1988. Longitudinal evolution of the Suez rift structure (Egypt). Tectonophysics 153, 221–233.

Cowie, P.A., Scholz, C.H., 1992. Physical explanation for the displacement-length relationship of faults using a post-yield fracture mechanics model. Journal of Structural Geology 14, 1133–1148.

Dauteuil, O., Brun, J.P., 1993. Oblique rifting in a slow-spreading ridge. Nature 361, 145–148.

Davy, P., Cobbold, P.R., 1991. Experiments on shortening of a 4-layer model on the continental lithosphere. Tectonophysics 188, 1–25.

Dubois, A., Odonne, F., Massonnat, G., Lebourg, T., Fabre, R., 2002. Analogue modelling of fault reactivation: tectonic inversion and oblique remobilisation of grabens. Journal of Structural Geology 24, 1741–1752.

Faccenna, C., Nalpas, T., Brun, J.P., Davy, P., 1995. The influence of pre-existing thrust fault on normal fault geometry in nature and in experiments. Journal of Structural Geology 17, 1995.

Gawthorpe, R.L., Leeder, M.R., 2000. Tectono-sedimentary evolution of active extensional basins. Basin Research 12, 195–218.

Higgins, R.I., Harris, L.B., 1997. The effect of cover composition on extensional faulting above re-activated basement faults: results from analogue modelling. Journal of Structural Geology 19, 89–98.

Hubbert, M.K., 1937. Theory of scale models as applied to the study of geologic structures. Geological Society of America Bulletin 48, 1459–1520.

Jarrigue, J.J., d'Estevou, P.O., Burollet, P.F., Montenat, C., Prat, P., Richert, J.P., Thiriet, J.P., 1990. The multistage tectonic evolution of the Gulf of Suez and northern Red Sea continental rifting from field observations. Tectonics 9, 441–465.

Krantz, R.W., 1991. Measurements of friction coefficients and cohesion for faulting and fault reactivation in laboratory models using sand and sand mixtures. Tectonophysics 188, 203–207.

Lavier, L.L., Buck, W.R., Poliakov, A.N.B., 1999. Self-consistent rolling-hinge model for the evolution of large-offset low-angle normal faults. Geology 27, 1127–1130.

Lezzar, K.E., Tiercelin, J.J., LeTurdu, C., Cohen, A.S., Reynolds, D.J., LeGall, B., Scholz, C.A., 2002. Control of normal fault interaction on the distribution of major Neogene sedimentary depocenters, Lake Tanganyika, East African rift. AAPG Bulletin 86, 1027–1059.

Lyberis, N., 1988. Tectonic evolution of the Gulf of Suez and the Gulf of Aqaba. Tectonophysics 153, 209–220.

Marchal, D., Guiraud, M., Rives, T., Van den Driessche, J., 1998. Space and time propagation processes of normal faults, in: Jones, G., Fisher, Q.J., Knipe, R.J. (Eds.), Faulting, Fault Sealing and Fluid Flow in Hydrocarbon Reservoirs Geological Society of London Special Publication, 147, pp. 51–70.

McClay, K., Khalil, S., 1998. Extensional hard linkage, eastern Gulf of Suez, Egypt. Geology 26, 563–566.

McClay, K.R., White, M.J., 1995. Analogue modelling of orthogonal and oblique rifting. Marine and Petroleum Geology 12, 137–151.

Michon, L., Merle, O., 2000. Crustal structures of the Rhine graben and the Massif Central grabens: an experimental approach. Tectonics 19, 896–904.

Morley, C.K., 1999. How successful are analogue models in addressing the influence of pre-existing fabrics on rift structure? Journal of Structural Geology 21, 1267–1274.

Morley, C.K., Haranya, C., Phoosongsee, W., Pongwapee, S., Kornsawan, A., Wonganan, N., 2004. Activation of rift oblique and rift parallel pre-existing fabrics during extension and their effect on deformation style: examples from the rifts of Thailand. Journal of Structural Geology 26, 1803–1829.

Moustafa, A.R., Abd-Allah, A.M., 1992. Transfer zones with en echelon faulting at the northern end of the Suez rift. Tectonics 11, 499–506.

Patton, T.L., Moustafa, A.R., Nelson, R.A., Abdine, S.A., 1994. Tectonic evolution and structural setting of the Suez rift, in: Landon, A.R. (Ed.), Interior Rift Basins AAPG Memoir, 59. The American Association of Petroleum Geology, Tulsa, pp. 9–55.

Peacock, D.C.P., Sanderson, D.J., 1991. Displacements, segment linkage and relay ramps in normal fault zones. Journal of Structural Geology 13, 721–733.

Ranalli, G., Yin, Z.M., 1990. Critical stress difference and orientation of faults in rocks with strength anisotropies: the two-dimensional case. Journal of Structural Geology 12, 1067–1071.

Sassi, W., Colletta, B., Balé, P., Pacquereau, T., 1993. Modelling of structural complexity in sedimentary basins: the role of pre-existing faults in thrust tectonics. Tectonophysics 226, 97–112.

Schütz, K.I., 1994. Structure and stratigraphy of the Gulf of Suez, Egypt, in: Landon, S.M. (Ed.), AAPG Memoir 59: Interior Rift Basins The American Association of Petroleum Geology, Tulsa, pp. 57–96.

Tron, V., Brun, J.P., 1991. Experiments on oblique rifting in brittle-ductile systems. Tectonophysics 188, 71–84.

Trudgill, B., Cartwright, J.A., 1994. Relay-ramp forms and normal-fault linkage, Canyonlands National Parks, Utah. Geological Society of America Bulletin 106, 1143–1157.

Vendeville, B., Cobbold, P.R., Davy, P., Brun, J.P., Choukroune, P., 1987. Physical models of extensional tectonics at various scales, in: Coward, M.P., Dewey, J.F., Hancock, P.L. (Eds.), Continental Extensional Tectonics Geological Society of London Special Publication, 28, pp. 95–107.

Weijermars, R., 1986. Flow behavior and physical chemistry of bouncing putties and related polymers in view of tectonic laboratory applications. Tectonophysics 124, 325–328.

Willemse, E.J.M., 1997. Segmented normal fault: correspondence between three-dimensional mechanical models and field data. Journal of Geophysical Research 102, 675–692.

Willemse, E.J.M., Pollard, D.D., Aydin, A., 1996. Three dimensional analysis of slip distributions on normal fault arrays with consequences for fault scaling. Journal of Structural Geology 18, 295–310.

Withjack, M.O., Callaway, S., 2000. Active normal faulting beneath a salt layer: an experimental study of deformation patterns in the cover sequence. AAPG Bulletin 84, 627–651.

Yin, Z.M., Ranalli, G., 1992. Critical stress difference, fault orientation and slip direction in anisotropic rocks under non-Andersonian stress systems. Journal of Structural Geology 14, 237–244.